Original Article

Spectroscopic Analysis, Electromagnetic Interaction And Molecular Docking Investigation Of Isopropylcyclohexane

R.Elayaraja[a] , M.Karnan [b] , S.Sindhuja[c] , M.Murali [c]

a. Department of Physics, Sri Meenakshi Vidiyal Arts and Science College-(Affiliated to Bharathidasan University –Trichirappalli, Tamil Nadu, India-621305)
b. PG & Research Department of Physics, Srimad Andavan Arts and Science College (Autonomous) – (Affiliated to Bharathidasan University – Trichirappalli, Tamil Nadu, India-620 005)
c. Department of Physics, Cauvery College for Women (Autonomous) - Affiliated to Bharathidasan University –Trichirappalli, Tamil Nadu, India-620 018)
c. Department of Physics, Saranathan College of Engineering - Affiliated to Anna University –Chennai, Tamil Nadu, India-620 012.
Corresponding author: elayaphysics@gmail.com
DOI: 10.47750/pnr.2022.13.S08.43

Abstract

Crystallographic, experimental (FT-IR and FT-Raman) and theoretical density function theory (DFT) and UV–Vis spectra of isopropylcyclohexane were investigated. The optimized geometry of the compound was calculated from the DFT–B3LYP gradient calculations employing 6-31G (d,p) and 6-311g basis set. The vibrational frequencies was evaluated via comparison with experimental values. Molecular stability has been analyzed using natural bond orbital (NBO) and natural localized molecular orbital (NLMO) analysis.The limits of the molecular electrostatic potential (MEP) was explained. The calculated HOMO and LUMO energies show the charge transfer occurs within the molecule .Molecular Docking studies of the molecule were carried out.

1. Introduction

Isopropylcyclohexane is one of the most studied cyclohexane it is easy to process, chemically stable, and its synthetic applications have been a constant matter of investigation for so many years [1]. Isopropylcyclohexane belongs to a class of cyclohexane compounds containing a six -membered ring made up of hydrogen with the formula C9H18 [2]. In medicinal chemistry isopropylcyclohexane derivatives have been well known for their medical applications. The normal isopropylcyclohexane are stable liquids which is very similar to the benzene compounds in the character like boiling point and in smell [3].Isopropylcyclohexane has a structure that is analogous to structure is like extremely reactive benzene derivative. [4] In most cases, the 2nd and 5th position of isopropylcyclohexane have been used for the polymerization [5]. The modification of the molecules for special electronic properties is operated on the 3rd and 4th -positions [6]. Isopropylcyclohexane are part of many organic compounds [7] having vast applications in the field of electronics and optoelectronics, medicine and materials [8]. The remarkable pharmacological efficiency of the compounds containing a cyclohexane ring in their structure is known for their antidepressant, anticonvulsant, antihistaminic, anaesthetic, antipuritic, analgesic action [9]. Isopropylcyclohexane and its derivatives exhibit diverse biological properties such as nemoticidal [10], insecticidal , antibacterial, antifungal, antiviral and antioxidant activity [11].

Density functional theory (DFT) approaches, especially those using hybrid functional, have evolved to a powerful and very reliable tool, being routinely used for the determination of various molecular properties [12]. B3LYP functional has been shown to provide an excellent compromise between accuracy and computational spectra for molecules of large and medium size [13]. The aim of the present study is to give a complete description of the molecular geometry and molecular vibrations of the title molecule. For that purpose, quantum chemical computations were carried out on title molecule using DFT. The calculated HOMO (Highly occupied molecular orbital's) and LUMO (Lowest Unoccupied molecular orbital's) energies show that charge transfer occurs in the title molecule.

DFT calculations are characterized to give very good vibrational frequencies of organic compounds if the calculated frequencies, are scaled to indemnify correlation, for basis set deficits and for not simple harmonic [14]. Molecular docking of the structure and calculate the protein of the molecule.[15

2. Experimental details

The Fourier transform infrared (FT-IR) spectrum of the pelletized was recorded at room temperature in the region 4000–400 cm^{-1} using Perkin–Elmer spectrum RX1 spectrophotometer equipped with composition of the pellet. The signals were collected a scan interval of 1cm^{-1} and at optical resolution of 0.4 cm^{-1}. The Fourier transform Raman (FT-Raman) BRUKER-RFS 27 spectrometer was used for the Raman spectral measurements at room temperature. The spectrometer consisted of a quartz beam splitter and a high sensitive germanium diode detector cooled to the liquid nitrogen temperature. The sample was packed in a glass tube of about 5 mm diameter and excited in the 180º geometry with 1064 nm laser line at 100mW power from a diode pumped air cooled Nd:YAG laser as an excitation wavelength in the region 4000–100 cm^{-1}

3. Computational details

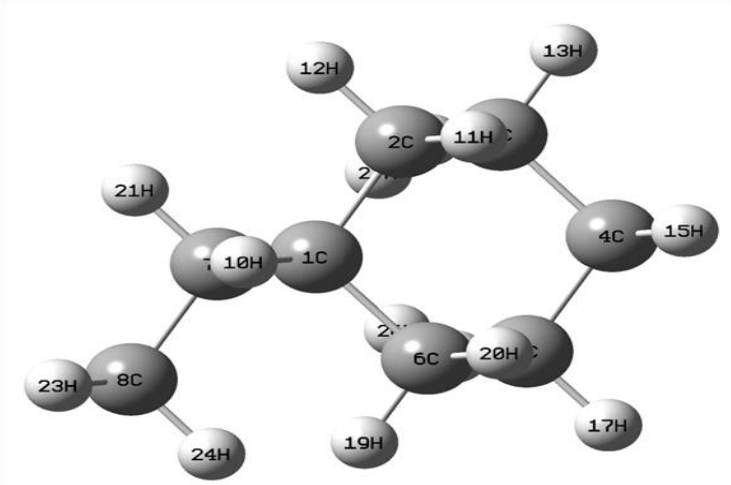

Fig. 1 Optimized structure of isopropylcyclohexane

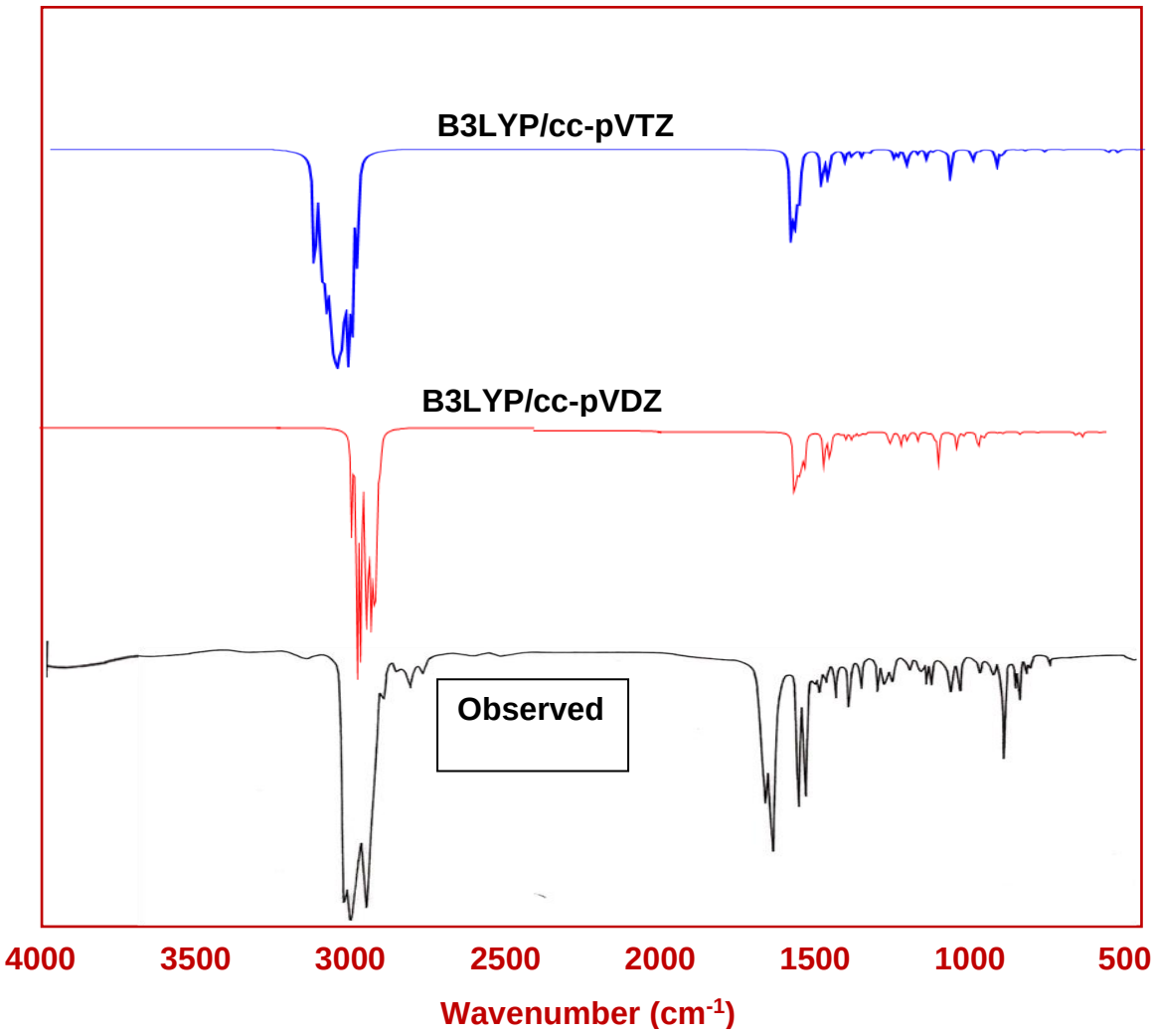

Fig.2 Observed and simulated FT-IR spectra of isopropylcyclohexane

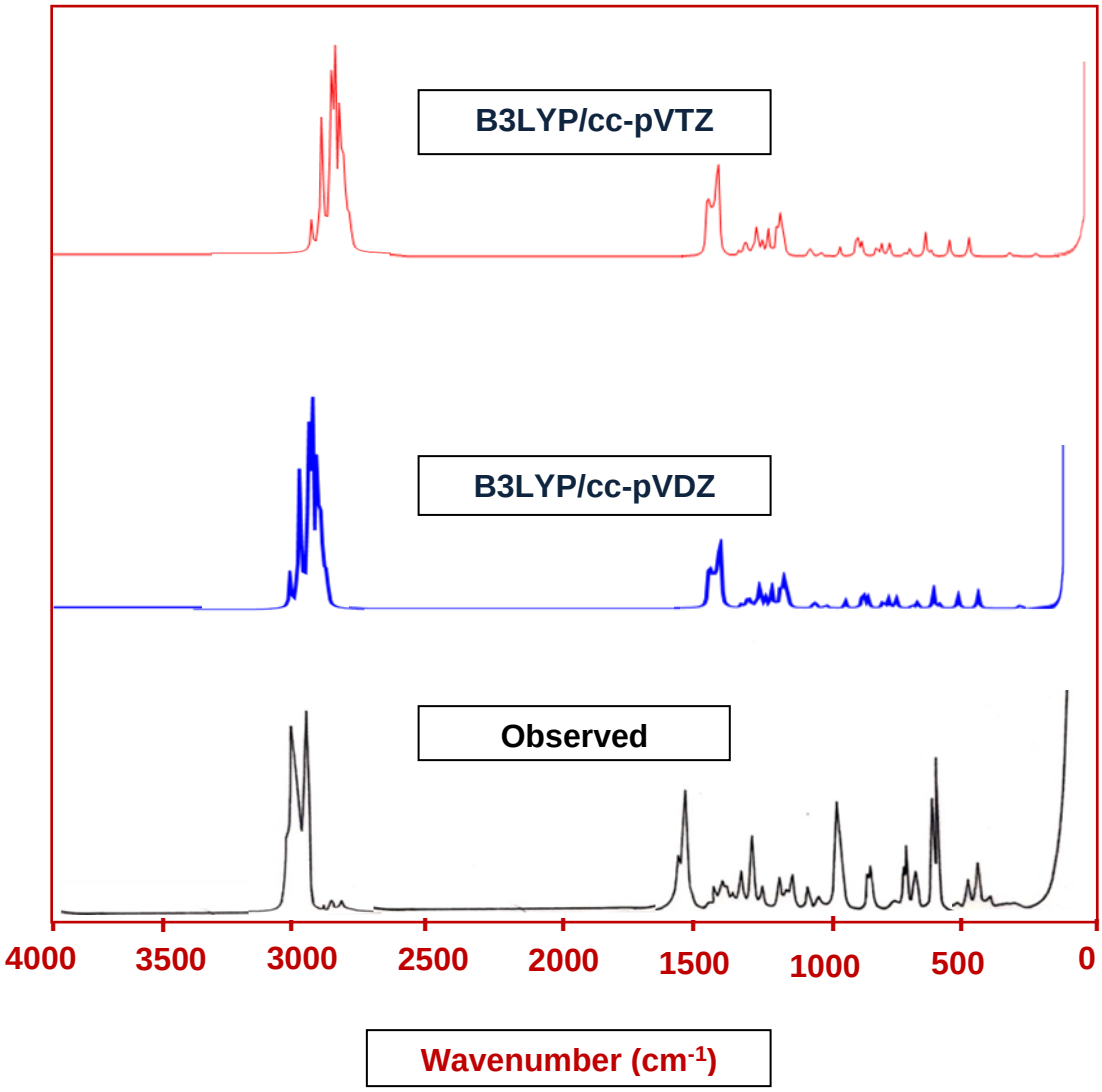

Fig.3 Observed and simulated FT-Raman spectra of isopropylcyclohexane

All DFT calculations of the title compound were carried out using Gaussian 09 program package using default thresholds and parameters [16]. The ground state structural geometries were fully optimized at the B3LYP method along with the standard 6-31g and 6-311g basis sets.

In the DFT calculations the Lee, Yang and Parr correlation functional is used together with Beck's three parameters exchange functional B3LYP. The geometry optimization was performed at the B3LYP density functional theory with the same basis set [17]. Harmonic vibrational frequencies were computed at the same level of theory. Structural analysis of the molecules has been executed to have an idea about the lowest energy structures of the category [18]. The molecular geometry has not been limited and all the calculations (vibrational wave numbers, optimized geometric parameters and other molecular properties) have been performed using the Gauss View molecular visualization program and the Gaussian 09W program package. The chemical reactivity behavior of the compound was predicted on the basis of reactivity indices obtained by HOMO and LUMO energy Eigen values. Molecular electrostatic potential (MEP) plot has been presented to know about the different sites of electrophilic and nucleophilic attacks of the compound.

3. Result's and Discussion & Vibrational analysis

The title molecule has 27 atoms with the molecular formula C9H18. The minimum energy configuration of the title molecule was again optimized at B3LYP/6-311G++ (d, p) level. The optimized stable geometry and the scheme of atom numbering of the compound . Isopropylcyclohexane is represented in Fig.1. The optimized structural parameters bond length, bond angle and the dihedral angle for the more stable geometry of the title compound is determined at B3LYP with 6-31g and 6-311g basis sets are presented in Table 1. The impact of the substituent on the molecular parameters, mainly in the C-C bond distance of ring carbon atoms seems to be varied. The mean bond length of aromatic ring is 1.40 Å. The longer bond length (1.48 Å) of C7-C9 is due to the absence of delocalization of carbonyl lone pair of electrons towards the ring.[19].The observed and calculated FTIR and FT-Raman spectra of Isopropylcyclohexane one are shown in Figs. 2 and 3 respectively. The observed FTIR and FT-Raman peak's wave numbers along with the theoretical IR and Raman wave numbers peak's are summarized in Table 2.[20].In the case of isopropylcyclohexane two C-H stretching vibrations are attributed, one is fell in higher wave number and another one is lower wave number. The C-H stretching wave numbers are observed by Kwiatowski et al, at 840 and 754 cm^{-1} whereas Kupta et al. [21] have been predicted theoretically at 2149 and 2910 cm^{-1} by DFT method. In our present study, , the C-CH bond lengths are 1.52 & 1.52 Å for C1-C2 and C3-C4 which are inside the ring. The ring connected C–H bond stretching vibration is calculated 4000 cm^{-1}. The identification of C–H vibrations is very difficult because of the interference of many bands in the area where the vibration of this bond happens.[22]For our title molecule, the C-H stretching appears in the region 4000-400 cm^{-1} and the observed wave number (4000 cm^{-1}) is coinciding very well with calculated wave number (4000 cm^{-1}) in FT-IR. The electronegative nitrogen atom makes the carbon atom more positive and the polar -CH group has effect on the adjacent bond. C=N and N-N and each has a well-known characteristic vibrational frequency of its own parameters. C-H stretching vibration, which due to its symmetry has a very characteristic and they are difficult to observe in the infrared spectrum. Because of the change in dipole moment, the C-H bond length in the

molecule also change in which has two abnomal C=H parts. These bands shift in wave
number and intensity in a different way depending on the neighboring groups, H-bonding [23]. The substituent's of title compound influence both the wave number and intensity. The medium band in FT-IR at 1234 cm-1 is accredited to the N-N stretching vibration of the molecule. The theoretical calculation by B3LYP method predicts the above said vibration at 1234 cm^{-1} exactly correlates with experimental findings

S.No	Parameter	Bond Length		Parameter	Bond Angle		Parameter	Bond Angle		Parameter	Dihedral Angle		Parameter	Dihedral Angle	
		6-31G	6-311G		6-31G	6-311G		6-31G	6-311G		6-31G	6-311G		6-31G	6-311G
1	C1-C2	1.55	1.55	C2-C1-C6	110.7	110.8	H17-C5-	107.3	106.39	C6-C1-C2-C3	46.33	44.87	C1-C2-C3-H14	66.95	69.57
2	C1-C6	1.55	1.55	C2-C1-C7	114.1	114.3	C1-C6-C5	114.8	115.35	C6-C1-C2-H11	-	-75.31	H11-C2-C3-C4	65.87	68.22
3	C1-C7	1.56	1.56	C2-C1-	105.3	105.2	C1-C6-H19	109.8	110.05	C6-C1-C2-H12	170.8	169.89	H11-C2-C3-	-55.42	-53.54
4	C1-H10	1.10	1.09	C6-C1-C7	115.5	115.6	C1-C6-H20	107.6	107.65	C7-C1-C2-C3	-	-88.05	H11-C2-C3-	-	-170.15
5	C2-C3	1.54	1.54	C6-C1-	106.0	105.9	C5-C6-H19	109.9	109.84	C7-C1-C2-H11	154.1	151.75	H12-C2-C3-C4	-	-176.59
6	C2-H11	1.09	1.09	C7-C1-	103.8	103.5	C5-C6-H20	107.4	107.64	C7-C1-C2-H12	38.36	36.96	H12-C2-C3-	60.85	61.63
7	C2-H12	1.09	1.09	C1-C2-C3	115.0	115.7	H19-C6-	106.7	105.79	H10-C1-C2-C3	160.6	158.97	H12-C2-C3-	-56.91	-54.97
8	C3-C4	1.54	1.53	C1-C2-	107.6	107.6	C1-C7-C8	110.1	110.88	H10-C1-C2-	40.93	38.78	C2-C3-C4-C5	58.68	56.46
9	C3-H13	1.09	1.09	C1-C2-	109.1	109.2	C1-C7-C9	116.5	116.60	H10-C1-C2-	-	-76.00	C2-C3-C4-H15	-61.36	-64.09
10	C3-H14	1.09	1.09	C3-C2-	107.4	107.4	C1-C7-H21	105.8	105.31	C2-C1-C6-C5	-	-44.30	C2-C3-C4-H16	-	178.93
11	C4-C5	1.54	1.53	C3-C2-	110.2	110.1	C8-C7-C9	108.9	109.54	C2-C1-C6-H19	-	-	H13-C3-C4-C5	179.39	177.66
12	C4-H15	1.09	1.09	H11-C2-	107.0	106.0	C8-C7-H21	107.3	106.80	C2-C1-C6-H20	74.21	75.88	H13-C3-C4-	59.34	57.10
13	C4-H16	1.09	1.09	C2-C3-C4	110.4	111.2	C9-C7-H21	107.6	107.09	C7-C1-C6-C5	86.30	87.94	H13-C3-C4-	-58.72	-59.86
14	C5-C6	1.54	1.54	C2-C3-	109.1	109.1	C7-C8-H22	110.4	110.70	C7-C1-C6-H19	-	-36.99	H14-C3-C4-C5	-62.98	-65.95
15	C5-H17	1.09	1.094	C2-C3-	110.4	110.6	C7-C8-H23	110.9	111.32	C7-C1-C6-H20	-	-	H14-C3-C4-	176.95	173.43
16	C5-H18	1.09	1.09	C4-C3-	110.1	110.1	C7-C8-H24	110.6	111.49	H10-C1-C6-C5	-	-	H14-C3-C4-	58.88	56.51
17	C6-H19	1.09	1.09	C4-C3-	109.1	109.2	H22-C8-	108.3	107.84	H10-C1-C6-	76.17	77.08	C2-C3-H14-	-34.59	-34.21
18	C6-H20	1.09	1.09	H13-C3-	107.3	106.2	H22-C8-	107.9	107.41	H10-C1-C6-	-	-37.77	C4-C3-H14-	87.11	88.57
19	C7-C8	1.54	1.54	C3-C4-C5	110.1	110.8	H23-C8-	108.3	107.88	C2-C1-C7-C8	-	-	H13-C3-C14-	-	-152.60
20	C7-C9	1.54	1.54	C3-C4-	109.1	109.2	C7-C9-H25	109.4	109.84	C2-C1-C7-C9	76.49	75.21	C3-C4-C5-C6	-58.23	-56.36
21	C7-H21	1.10	1.09	C3-C4-	110.3	110.3	C7-C9-H26	110.7	111.40	C2-C1-C7-H21	-	-43.34	C3-C4-C5-H17	-	-177.65
22	C8-H22	1.09	1.09	C5-C4-	109.3	109.3	C7-C9-H27	111.9	112.45	C6-C1-C7-C8	71.11	70.87	C3-C4-C5-H18	63.59	66.02
23	C8-H23	1.09	1.09	C5-C4-	110.2	110.2	H25-C9-	107.8	107.29	C6-C1-C7-C9	-	-55.39	H15-C4-C5-C6	61.71	64.12
24	C8-H24	1.09	1.09	H15-C4-	107.6	106.6	H25-C9-	108.0	107.48	C6-C1-C7-H21	-	-	H15-C4-C5-	-59.01	-57.17
25	C9-H25	1.09	1.09	C4-C5-C6	111.1	111.7	H26-C9-	108.6	108.12	H10-C1-C7-C8	-	-44.56	H15-C4-C5-	-	-173.48
26	C9-H26	1.09	1.09	C4-C5-	110.0	110.0	C3-H14-	131.4	128.90	H10-C1-C7-C9	-	-	H16-C4-C5-C6	179.81	-178.88

27	C9-H27	1.09	1.08	C4-C5-	108.9	108.9	C5-H18-	126.4	125.85	H10-C1-C7-	71.11	70.60	H16-C4-C5-	59.08	59.82
28	H14-H27	2.04	2.10	C6-C5-	108.9	109.0	C9-H26-	108.7	109.76	C1-C2-C3-C4	-	-52.04	H16-C4-C5-	-58.36	-56.49
29	H18-H26	2.15	2.22	C6-C5-	110.3	110.4	C9-H27-	134.2	134.12	C1-C2-C3-H13	-	-	C4-C5-C6-C1	52.63	51.36

Table 1: **Experimental and Calculated B3LYP/ 6-31g and B3LYP/6-311g levels of vibrational frequencies (cm^{-1}), of Isopropylcyclohexane**

Table 2: **Experimental and Calculated B3LYP/ 6-31g and B3LYP/6-311g levels of vibrational frequencies (cm^{-1}), of Isopropylcyclohexane**

S.No	Observed frequency		Calculated Frequency				Vibrational Assignments
	FT-IR	FT-Raman	Unscaled		Scaled		
			6-31G	6-311G	6-31G	6-311G	
1			3142	3105	3135	3100	υC H_3 (80)
2	3110		3119	3077	3110	3075	υas CH_2 (80) υCH_2 (10)
3			3109	3076	3100	3050	υas CH_2 (60) υas CH_2 (20) υas CH_2 (10)
4			3108	3069			υas CH_2 (70) υas CH_2 (10)
5			3102	3060			υas CH_2 (70) υas CH_2 (10)
6			3099	3046			υas CH_2 (70) υas CH_2 (10)
7			3076	3039			υas CH_2 (70) υas CH_2 (10) υas CH_2 (10)
8			3074	3036			ʈ CH_2 (80) υas CH_2 (10)
9			3066	3027			υas CH_2 (80) υas CH_2 (10)
10			3055	3016			υas CH_2 (70) υas CH_2 (10) υas CH_2 (10)
11			3052	3011			υas CH_3 (70) υas CH_2 (10) υas CH_2 (10)
12			3050	3005			υCH_3 (70) υas CH_2 (10)
13			3043	3005	3035	2990	υCH_3 (80) υas CH_2 (10) ʈ CH_2 (90)
14			3038	2998			υ CH_2 (70) υas CH_2 (10)
15			3031	2985	3025	2980	υ CH_2 (80) υas CH_2 (10)
16			3027	2984			υCH_2 (80)
17	2980	2780	3020	2969	3010	2960	υ CH_2 (80)
18	2960	2730	3008	2963	2990	2950	υ CH_2 (90)
19	2860	2750	1579	1553	1575	1503	υas CH_2 (80)
20	2810	2710	1578	1549	1570	1535	υ CH_2 (70)
21	2580		1566	1541			υ CH_2 (70) wag CH_2 (10)
22	2640		1564	1538			υCH_2 (70) υas CH_2 (10) rock CH_2 (10)
23	2750		1557	1536	1550	1525	rockCH_3 (80) CH_2 (80)
24			1550	1527			δCH_3 (80)
25			1547	1526			δCH_3 (80) δ CH_2 (10)
26			1542	1526			δCH_3 (80) δ CH_2 (10)
27		1470	1540	1523			δ CH_2 (80) δCH_2 (10)
28	1450	1450	1468	1453	1460	1425	δCH_3 (80)
29			1450	1437			δCH_3 (80) δCH_2 (10)
30			1442	1431			δCH_2 (80)
31			1432	1422			δ CH_2 (80)
32	1420		1420	1413			δ CH_2 (80)
33			1409	1399	1400	1390	δ CH_2 (80)
34			1407	1397			δCH_3 (80)
35			1399	1388			δC CH_2 (80) δ CH_2 (10)
36			1386	1379	1380	1370	wag CH_2 (80)
37		1360	1366	1356			wag CH_2 (80)
38	1350	1340	1354	1342	1350	1337	wag CH_2 (80)wagCH_3 (10)
39		1330	1334	1323			wag CH_2 (80)wagCH_3 (10)
40	1320	1320	1321	1309			rock CH_2 (80)
41	1280	1310	1312	1298			rock CH_2 (80)

42	1270	1300	1222	1218	1220	1200	wag CH_2 (90)
43	1260	1280	1215	1205			wag CH_2 (80)wagC CH_2 (10)
44	1250	1270	1186	1178			rock CH_2 (90)
45	1230	1250	1177	1167	1170	1159	ъ CH_2 (90)
46	1210	1230	1153	1141			wag CH_2 (80)wagCH_3 (10)
47	1200	1180	1113	1112			wag CH_2 (80)wagCH_3 (10)
48	1180	1150	1074	1091	1065	1085	rock CH_2 (80)
49	1130	1100	1055	1060			ъ CH_2 (80)
50	1120	1090	1049	1051			inplaneъCH3(80) ъ CH_2 (10)
51	1110	1080	1036	1034	1025	1030	ъ CH_2 (80) ъCH_3 (10)
52	1100	1050	984	980	980	975	rockCH_3 (70) rockCH_3 (10)
53	1010	980	966	962			rockCH_3 (80)
54	980		964	958			rockCH_3 (70) rockCCH_2 (10) rockCH_3 (10)
55	920	940	940	941	934	938	wag CH_2 (90)
56	900	900	885	884	880	882	δ CH_2 (80)
57			867	872			ъ CH_2 (90)
58	860	860	860	865			δ CH_2 (80) δCCH_3 (10)
59	840	840	812	815	805	812	ъ CH_2 (90)
60	820	820	793	790			δ CH_2 (80)
61	780	780	727	728	715	720	ъ CH_2 (80) ъCH_3 (10)
62	760	620	659	663	650	658	δ CH_2 (80)
63	680	580	515	521	500	515	δCH_2 (80) δC CH_2 (10)
64	510	498	491	488			rockCH_3 (70) rockCCH_2 (10) rock CH_2(10)
65		490	426	428	410	415	δCH_2 (80)
66		488	421	418			δ CH_2 (80)
67	380	472	357	349	350	344	wagCH_3 (80)wagCH_3(10)
68		350	327	320			δ CH_2 (80) δC CH_2 (10)
69		330	309	290	300	280	rock CH_2 (80)
70		310	270	255	265	250	δCH2(80) §CH_3 (10)
71			260	252	250	245	wagCH_3 (70)wagCH_3 (10)wagCCH_2 (10)
72			242	218	231	210	ъ CH_2 (80) ъC CH_2 (10)
73		150	195	185	188	176	rock CH_2 (80) rockCH_3 (10)
74			132	127	125	115	rock CH_2 (80) rock CH_2 (10)
75			51	46	40	38	δ CH_2 (80) §CH_3 (10)

4. VIBRATIONAL ANALYSIS

The titled molecule under investigation has 27 atoms and has 75 normal modes of fundamental vibrations. Vibrational wave numbers for all the fundamental modes of the titled compound were computed using DFT (B3LYP) methods with 6-311++G (d,p) basis set. The DFT values along with the experimental values are jointly presented. The experimental and theoretical spectra of the titled compound are shown in Fig. 2 and 3, respectively.

By observing the experimental and theoretical frequencies, the theoretical values were slightly higher than the experimental values for the majority of the normal modes, comes to the conclusion that two factors may be responsible for the discrepancies between the experimental and computed wave numbers; the first is caused by the unpredictable electronic distribution among the different bonds in the molecule [24] and the second reason is the enharmonic nature of the vibrations which cannot be accounted completely by the theory. To make coincidence with experimental and theoretical data, scaling strategies were utilized.

C-C and C-H vibrations

The aromatic ring vibrational modes of the title molecule have been verified based on the vibrational spectra of previously published vibrations of the benzene molecule which helpful in the identification of the phenyl ring modes [25]. The ring stretching vibrations is very prominent, as the double bond is in conjugation with the ring, in the vibrational spectra of benzene and its derivatives [26]. The ring carbon-carbon stretching vibrations occur in the region 1650-1450 cm^{-1}. In the title compound, the wave numbers observed in the FT-IR spectrum at 1609, 1578, 1348, 1328 cm^{-1} have been assigned to C-C stretching vibrations. The theoretically computed values at 1610, 1576, 1515, 1345, 1326 cm^{-1} show the excellent agreement with the experimental data. The characteristic region for the identification of C-H stretching vibration, the heteroaromatic structure illustrated in the region 3100–3000 cm^{-1}. In the aromatic compounds, the C-H stretching normally occurs in the region of 3100- 3000 cm^{-1} [27]. For the title molecule, there are eight CH stretching vibrations of morpoline rings, which are theoretically observed at 3250, 3247, 3244, 3241, 3181, 3180, 3178 and 3174 cm^{-1}, all these are found completely within the range which shows they are not affected by the substitutional groups, as predicted in the earlier analyses.[28]

There are six CH bonds in the aliphatic groups; five in methoxy and one in aldehyde groups respectively. Some values are pushed up and some are pulled down, these are impact observed as due to the influence of hydrogen bonds. The calculated wave numbers of the C-H symmetric stretching vibrations using B3LYP/cc-pVDZ in title molecule at 3094, 3075, 3060, 3033, 3021, and 3010 $cm^{-1}$are in good agreement with the experimental data. The C–H in-plane bending and C–H out-of-plane bending vibrations are normally found in the range 1400–1000 and 1000–750 cm^{-1}, respectively in aromatic compounds and are very useful for characterization purposes [29]. The C-H in-plane bending vibrations are observed at 1484, 1421, 1375, 1296, 1156 cm^{-1} in FT-IR and the calculated wave numbers are 1483, 1420, 1376, 1295, 1155 cm^{-1} the same was around in the calculated. The C-H out-of-plane bending vibrations are calculated at 957, 910, 829, 685 cm-1. The experimental values are assigned at 957, 912, 828, 687 cm^{-1} which show excellent agreement with calculated ones.

5.Molecular Electrostatic Potential (MEP)

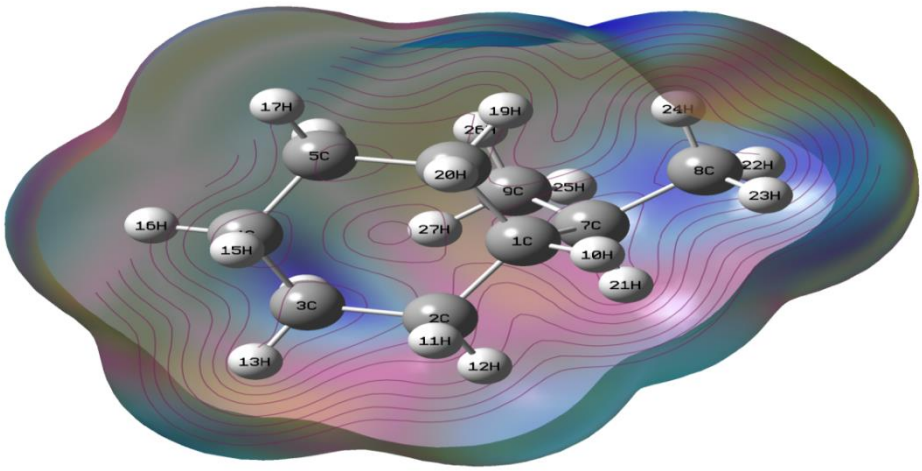

Molecular electrostatic potential mapping is very useful in the investigation of the molecular structure with its physiochemical

property relationships [30]. Molecular electrostatic potential surfaces are important in computer-aided drug design as a result of them assisting in optimization of electrostatic interactions between the protein and the ligand[31]. These surfaces are accustomed compare different inhibitors with substrates or transition states of the reaction. Electrostatic potential surfaces are either displayed as isocontour surfaces or mapped onto the

molecular electron density. The later are more widely used because they maintain the sense of underlying chemical structure better than isocontour plots. The MEP surface displays the molecular shape, size and electrostatic potential value. The color scheme for the MEP surface is partially negative charge or red-electron rich; partially positive charge or blue-electron deficient; yellow slightly electron rich region; light green-slightly electron deficient region, respectively. Potential increases in the order red < orange < yellow < green < blue. The MEP diagram of

shown in Fig. 4. The molecule must present atoms either with positive potential isosurface and atoms with negative potential isosurface. MEP is very helpful for the qualitative elucidation of electrophilic and nucleophilic reactions for the study of biological

discovery process and hydrogen bonding interactions [32]. An electron density iso-surface mapped with electrostatic potential surface depicts the size, shape, charge density and site of chemical reactivity of the molecule.

From the MEP picture, oxygen has higher electronegativity value than hydrogen and carbon. Oxygen atom would consequently possess higher electric density around it, than hydrogen and carbon atoms. Thus, the spherical region that corresponds to an hydrogen atom would have a red position on it. However, the light-yellow region spread on the MEP surface due to potential halfway between the two extreme regions and this confirms the existence of an intermolecular interaction. To predict the reactive sites of electrophilic and nucleophilic attack for the investigated molecule, the MEP obtained using the B3LYP/cc-pVDZ optimized geometry was calculated and the value is -7.150eV to 7.150 eV. The negative (red and yellow) regions of MEP were related to electrophilic reactivity and the positive (blue) regions corresponds to nucleophilic reactivity as shown. These are two possible sites of electrophilic attack. The negative regions are mainly localized on the carbonyl oxygen atoms and also a negative electrostatic potential region is observed around the hydrogen atom. The confirms the existence of an intermolecular C-H----H interaction between the protonated (addition of a proton (H+) to an atom or molecule) and unprotonated C & H atoms. The molecular electrostatic potential map shows that the positive potential sites is around the hydrogen atoms and negative potential sites are electronegative atoms. These sites give information about the region from where the compound can have noncovalent interactions.

5.1 Mulliken Charges

The calculation of atomic charges plays an important role in the application of quantum mechanical calculations to molecular systems. Mulliken charges are calculated by determining the electron population of each atom as defined in the basis functions. The charge distributions calculated by the Mulliken [33] and NBO methods for the equilibrium geometry of isopropylcyclohexane are given in Table. and the results can, however, better be represented in graphical form as depicted in. The charge distribution on the molecule has an important influence on the vibrational spectra. In the title compound, the distribution of Mulliken atomic charges shows the direction of delocalization and shows that the natural atomic charges are more sensitive to the changes in the molecular structure than Mulliken's net charge. Also we have done a comparison of Mulliken charges obtained by different basis sets and tabulated it in order to assess the sensitivity of the calculated charges to changes in (i) the choice of the basis set; (ii) the choice of the quantum mechanical method. We have observed a change in the charge distribution by changing different basis sets. Based on the charge distribution calculated by different basis sets it can be concluded that all the hetero atoms showed significant electron density. In isopropylcyclohexane an increased electron density(negative charge) can be also found at C1, C2, C3, C4, C5, C6, C7, C8, C9. Significantly positive charges were predicted for H10, H11, H12, H13, H14, H15, H16, H17, H18, H19, H20, H21, H22, H23, H24, H25, H26 for 631g, 6311g basis set.

Local reactive descriptors

Fukui function is one of the widely used local density functional descriptors to model chemical reactivity and site selectivity of the molecule. It is a local reactivity descriptor that indicates the preferred regions where a chemical species will change its density when the number of electrons is modified [34]. It is possible to define the corresponding condensed or atomic Fukui functions on j^{th} atom site as,

$$F_j^+ = q_j(N+1) - q_j(N)$$

$$F_j^- = q_j(N) - q_j(N-1)$$

$$F_j^0 = {}^1\!/_2\,[q_j(N+1) - q_j(N-1)]$$

for an electrophilic F_j^-, nucleophilic or free radical attack F_j^-, on the reference molecule, respectively. In these equations, q_j is the atomic charge (evaluated from mulliken population analysis, electrostatic derived charge, etc.) at the j^{th} atomic site is the neutral (N), anionic (N+1) or cationic (N-1) chemical species. The concept of generalized philicity almost all information about the known different global and local reactivity and selectivity descriptor, in addition to the information regarding electrophilic/ nucleophilic power of a given atomic site in a molecule. A dual descriptor ($\Delta f(r)$), which is defined as the difference between the nucleophilic and electrophilic Fukui function and is given by[35],

$$\Delta f(r) = [f^+(r) - f^-(r)]$$

$\Delta f(r) > 0$,hen the site is favored for a nucleophilic attack,

whereas if

$\Delta f(r) > 0$,, then the site may be favored for an electrophilic attack.

Under this situation, the reactivity descriptor $\Delta f(r)$provides useful information on both stabilizing and destabilizing interactions between a nucleophile and an electrophile and helps in identifying the electrophilic/nucleophilic behaviour of a specific site within a molecule. It provides positive value (i.e (i.e $\Delta f(r) > 0$)) for site prone for nucleophilic attack and a negative value (i.e $\Delta f(r) < 0$) prone for electrophilic attack and these values summarized.

Global reactivity descriptors

The energies of HOMO and LUMO are negative, which indicates that the studied compound is stable [36]. The HOMO and LUMO plots for the title compound. The HOMO and LUMO are localized over the rings the HOMO of π nature is delocalized over the C−C bonds of the phenyl ring and C−Cl groups. Accordingly, the HOMO-LUMO transition implies an electron density transfer from the phenyl ring to the Cl group. For understanding various aspects of pharmacological sciences including drug design and the possible eco-toxicological characteristics of the drug molecules, several new chemical reactivity descriptors have been proposed. Conceptual DFT based descriptors have helped in many ways to understand the structure of the molecules and their reactivity by calculating the chemical potential, global hardness and electrophilicity. Using HOMO and LUMO orbital energies, the ionization energy and electron affinity can be expressed as:$I = -E_{HOMO}$, $A = -E_{LOMO} = (\eta = (-E_{HOMO} + E_{LOMO})/2$ and $\mu = (E_{HOMO} + E_{LOMO})/2$. The Electronegativity (χ) and hardness (η) evaluation are defined as $\chi = (I + A)/2$ and $\eta = (I - A)/2$ Electrophilicity index proposed by Par is a measure of energy lowering due to maximal electron flow between donor and acceptor. In terms of chemical potential (μ), they defined global electrophilicity index (ω) as $\omega = \mu^2/2\eta$. This index measures the stabilization in energy when the system acquired an additional electronic charge from the environment. Electrophilicity encompasses both the ability of an electrophile to acquire additional electronic charge and the resistance of the system to exchange electronic charge with the environment. It contains information about both electron transfer (chemical potential) and stability (hardness) and is a better descriptor of global chemical reactivity.

The calculated values of global reactive descriptors for the title compound are, I = 7.1252 eV, A = 2.0738 eV, η = 2.5257 eV, χ = 4.5995 eV and chemical potential, μ = -χ = -4.5995 eV. Electrophilicity index, $\omega = \mu^2/2\eta$ = 4.1879 eV is deduced from ionization energy and electron affinity values. Due to low value of electrophilicity index, indicate that the title compound is more reactive towards nucleophiles and it is seen that the chemical potential of the title compound is negative and it means that the compound is stable [37]. They do not decompose spontaneously into the elements they are made up of. The hardness signifies the resistance towards the deformation of electron cloud of chemical systems under small perturbation encountered during the chemical process. The principle of hardness works in chemistry and physics but it is not physically observable. Soft systems are large and highly polarisable, while hard systems are relatively small and much less polarisable.

6. Frontier Molecular Orbital's

Highly occupied molecular orbital (HOMO) and Lowest unoccupied molecular orbital (LUMO) are the main orbital that take part in chemical stability. Molecular orbital's can provide insight into the nature of reactivity and some of the structural and physical properties. The HOMO represents the ability to donate an electron, while LUMO as an electron acceptor represents the ability to obtain an electron. The one electron excitation from HOMO and LUMO mainly described the electronic transition absorption correspond to the transition from ground to first excited state [38]. The energy gap between HOMO and LUMO has been used to prove the bioactivity from intermolecular charge transfer [39]. The energy gap measures the kinetic energy stability of the molecules. Considering the chemical hardness, large HOMO-LUMO gap means a hard molecule and small HOMO-LUMO gap means a soft molecule and also can relate the stability of the molecule to hardness, which means that increase of the HOMO-LUMO energy gap decreases reactivity of the compound that leads to increase in the stability of the molecule [40]. The frontier molecules orbital, HOMO and LUMO and frontier molecular energy gap helping the reactivity and kinetic stability of molecules are essential parameters in the electronic studies [41]. The energy values of HOMO (E_{HOMO}) and LUMO (E_{LUMO}) are -0.079 and 0.284 for 631-G , -0.033 and 0.291eV respectively. In the studied compound the HOMO-LUMO energy gap (ΔE) is 0.363 eV that reflects the chemical reactivity of the molecule. Using HOMO and LUMO orbital energies, the ionization energy and electron affinity can be expressed as: I = $-E_{HOMO}$ = 0.284 eV. A = $-E_{LUMO}$ = -0.079 eV. The hardness (η)= 0.181 ev and chemical potential (μ) -0.103ev chemical softness (S) 5.503,Global electrophilicity (ω) 0.029 ev are given the following formula η = (I-A)/2 and μ = -(I+A)/2, where I and A are the first ionization potential and electron affinity of the chemical species. For the 6311g title compound, EHOMO = 0.291 eV, ELUMO = -0.033 eV, Energy gap = HOMO-LUMO = 0.324 eV, Ionization potential (I) = 0.291 eV, Electron affinity (A) = 0.103 eV, Chemical hardness (η)

= 0.162 eV, Electronegativity (χ) = 0.126 eV, Softness (s) = 6.174 eV-1, Chemical potential (μ) = -0.129 eV, Electrophilicity index (ω) = 0.051eV

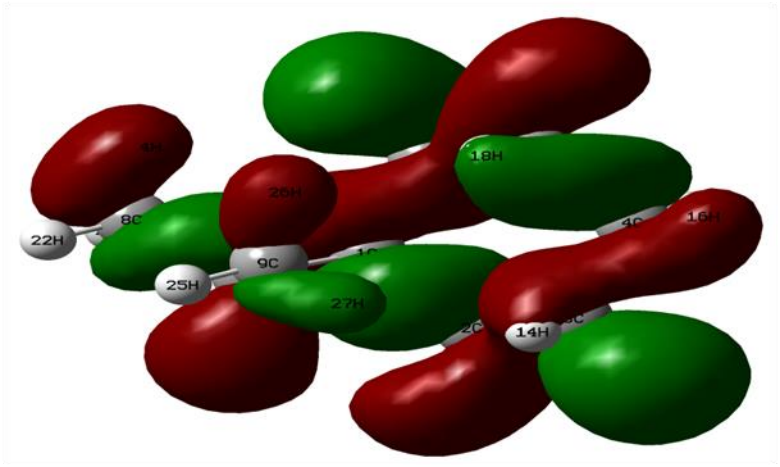

LUMO-

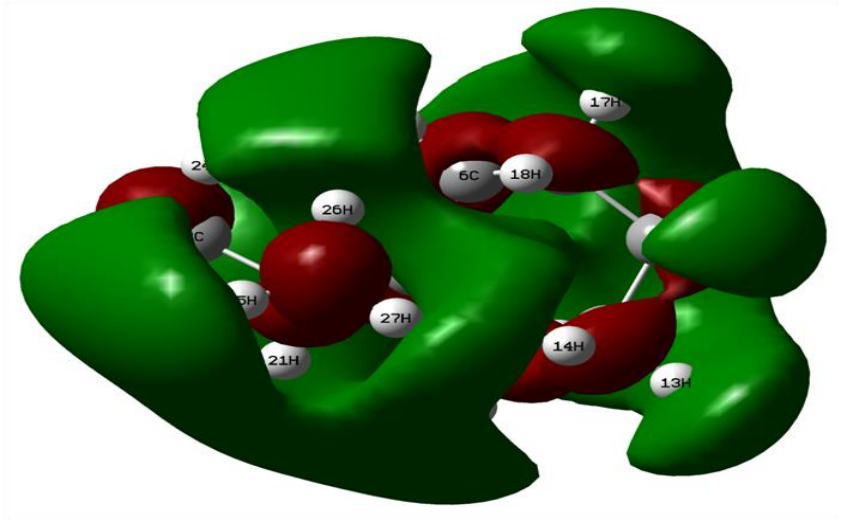

HOMO

Fig. 4. HOMO- LUMO plot of Isopropylcyclohexane

Electronic Property	B3LYP/6-31G	B3LYP/6-311G
EHOMO(eV)	0.284	0.291
ELUMO (eV)	-0.079	-0.033
Energy gap(eV)	0.363	0.324
Ionization potential (I)(eV)	0.284	0.291
Electron affinity (A)(eV)	0.103	0.129
Electro negativity (**χ**)	0.133	0.126
Global hardness (**η**)	0.182	0.162
Chemical potential (μ)	-0.103	-0.129
Chemical softness S (eV-1)	5.503	6.174
Global electrophilicity index (ω)	0.029	0.051

T**able 4: Frontier Molecular Orbital analysis of Isopropylcyclohexane at B3LYP/6-31G and B3LYP/6-311G**

7. Docking Analysis

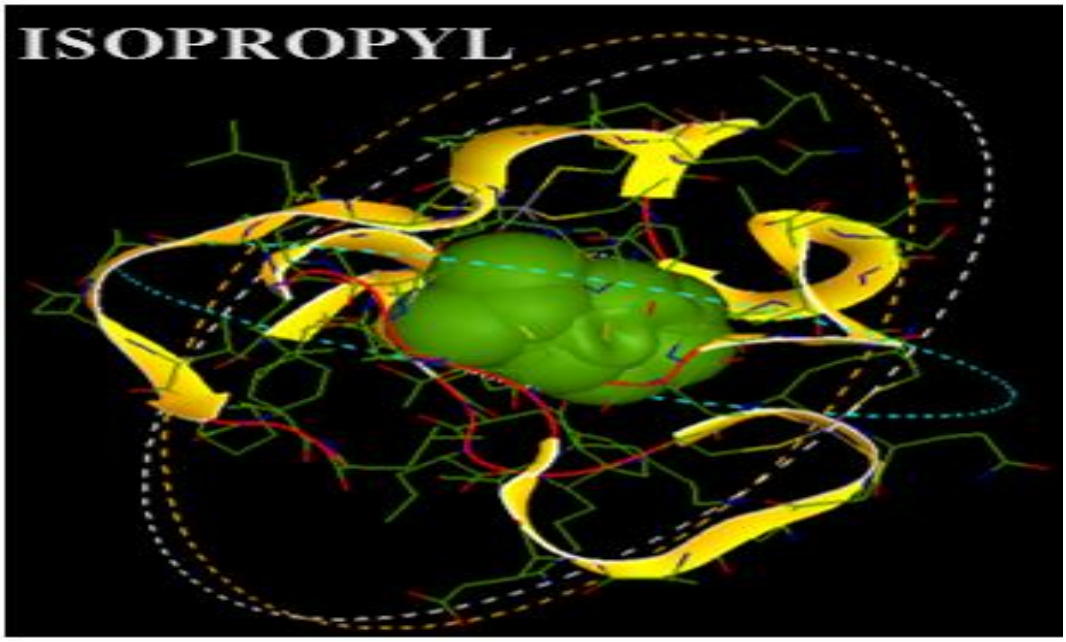

Docking studies (Software Details)

Docking studies of compounds () have been performed using HEX 6.1 software which is an interactive molecular graphics program for the drug – protein binding interaction. The structure of the complexes were sketched by CHEMSKETCH (http://www.acdlabs.com). The crystal structure of EGFR kinase domain (PDB ID: 1BOR (Blood Cancer) in complex with an

irreversible inhibitors was obtained from the protein data bank. Visualization of the docked poses has been done by using PyMOL software.

Molecular docking analysis of isopropylcyclohexane

The study of molecular docking of the present molecule was carried out by Auto Dock – Vina software and PyMol molecular graphics system [42]. The ligand was chosen by minimizing its energy at B3LYP/ 6-311G++ (d, p) functional and basis sets and the online tool "Pass" is used to predict the different types of biological activities of the title molecule. In this present study, Escherichia coli (protein ID: 2R9N). Generally, Hydrogen were added with target protein and therefore Kollman atomic charges were observed and Lamarckian genetic algorithm (LGA) was used for molecular docking study in Auto Dock software package. The binding pocket of protein was obtained by grid size of 90 X, 90 Y & 92 Z Å with the help of Auto grid. By using Auto dock software, the inhibition constants, intermolecular energy are calculated. The bond distance of the title molecule to the targeted protein were 1.8 with inhibition constant of three residue (LYS '183') involved in bonding with the title compound were obtained using Discover studio visualize 4.1 software and the values are tabulated in Table 8. The formation of hydrogen between ligands and protein were represented by yellow dotted lines in the Fig 10. In addition, the molecule is suggested with Homo sapiens activity which is consistent with the experimental values.

Protein (PDB ID)	Binding Energy	No. of hydrogen bond	Bonded Residues	Bond Distance
2R9N	-142.22	1	LYS 183	1.8

Conclusions:

In this paper we have reported a complete structural ,the FT-IR, FT-Raman studies were carried out for synthesized MPET. DFT calculations at the B3LYP/6-31G (d, p) and 6-311g level of theory were performed in order to analyze structural properties of MPET. The calculated structural parameters by the DFT method closely match with single crystal XRD data. MEP plays an important role in determining the stability of the molecule. The energies for the various possible conformers of the title compound was calculated and the minimum energy structure was chosen for the computational study as well as for Docking. From the Molecular docking studies, it shows that the positive potential isosurface of MPET are very active and also interact with protein target. Hence this MPET based new compound has also tested to estimate its potential against cholesterol biosynthesis. Vibrational and electronic properties of Isopropylcyclohexane by using experimental techniques (FT-IR,FT-Raman, UV–Vis absorption spectra, NMR spectroscopy and X-ray diffraction). The results showed no significant geometrical differences (distances and angles), when the solid state crystal structure is compared with the optimized structure in the gas phase theoretical method (DFT/B3LYP/6-31G (d,p)). Very good agreement between principal vibrational frequencies calculated from the optimized structure and the experimental spectroscopic data. The MEP map shows that the negative potential sites are on electronegative atoms as well as the positive potential sites are around the hydrogen atoms. The energies for the various possible conformers of the title compound was calculated and the minimum energy structure was chosen for the computational study as well as for Docking.

Reference:

1. DJ Zhang, PR Wang, ZC Mao, GJ Xu - Science China Earth Sciences
2. S Vitu, JN Jaubert, J Pauly, JL Daridon… - The Journal of Supercritical …,
3. C Alba, LE Busse, DJ List, CA Angell - The Journal of chemical …,
4. AE Shilov, GB Shul'pin - Chemical reviews,
5. A Lipatov, M Alhabeb, MR Lukatskaya… - Advanced Electronic …, 2016 - Wiley Online Library
6. GB Barlow, M Stacey, JC Tatlow - Journal of the Chemical Society …, 1955 - pubs.rsc.org
7. P Meredith, CJ Bettinger, M Irimia-Vladu… - Reports on Progress …, 2013 - iopscience.iop.org
8. RB Silverman - 2005 - books.google.com
9. S Grimme - … Interdisciplinary Reviews: Computational Molecular …, 2011 - Wiley Online Library
10. P Carbonniere, V Barone - Chemical physics letters, 2004 - Elsevier
11. R Rahmani, N Boukabcha, A Chouaih… - … of Molecular Structure, 2018 - Elsevier
12. GM Morris, M Lim-Wilby - Molecular modeling of proteins, 2008 - Springer
13. Y Mei-Rong, S Yu, X Yong-Jin - SpringerPlus, 2014 - Springer
14. G Sun, M Kertesz - New Journal of Chemistry, 2000 - pubs.rsc.org
15. JF Stanton, J Gauss, JD Watts… - … Journal of Quantum …, 1992 - Wiley Online Library
16. T Kupka, R Wrzalik, G Pasterna, K Pasterny - Journal of molecular structure, 2002 - Elsevier

17. DS Pal, H Kar, S Ghosh - Chemical Communications, 2018 - pubs.rsc.org
18. N Subramanian, N Sundaraganesan… - … Spectroscopy, 2010 - Elsevier
19. JP Abraham, D Sajan, V Shettigar… - Journal of Molecular …, 2009 - Elsevier
20. NK Howell, G Arteaga, S Nakai… - Journal of agricultural …, 1999 - ACS Publications
21. S Quillard, G Louarn, S Lefrant, AG MacDiarmid - Physical Review B, 1994 - APS
22. CF Matta, AA Arabi - Future medicinal chemistry, 2011 - Future Science
23. VR Mishra, CW Ghanavatkar, SN Mali… - Journal of …, 2019 - Taylor & Francis
24. **A** Srivastava, R Mishra, S Kumar, K Dev… - Journal of Molecular …, 2015 - Elsevier
25. G Naray-Szabo, GG Ferenczy - Chemical Reviews, 1995 - ACS Publications
26. RR Contreras, P Fuentealba, M Galván… - Chemical Physics Letters, 1999 - Elsevier
27. PK Chattaraj, B Maiti, U Sarkar - The Journal of Physical Chemistry …, 2003 - ACS Publications
28. M Rezaei-Sameti, P Zarei - Adsorption, 2018 - Springer
29. CS Abraham, JC Prasana, S Muthu - Spectrochimica Acta Part A: Molecular …, 2017 - Elsevier
30. M Belletête, M Bédard, M Leclerc… - Journal of Molecular …, 2004 - Elsevier
31. HS El-Sheshtawy, AM Abou Baker - Journal of Molecular Structure, 2014 - Elsevier
32. RG Pearson - Journal of Chemical Sciences, 2005 - ias.ac.in